

Critical exponents of correlated percolation of sites not visited by a random walk

Raz Halifa Levi^{1,*} and Yacov Kantor²

¹The Faculty of Engineering, Tel Aviv University, Tel Aviv 6997801, Israel

²School of Physics and Astronomy, Tel Aviv University, Tel Aviv 6997801, Israel

 (Received 8 May 2024; accepted 22 July 2024; published 8 August 2024)

We consider a d -dimensional correlated percolation problem of sites *not* visited by a random walk on a hypercubic lattice L^d for $d = 3, 4$, and 5 . The length of the random walk is $\mathcal{N} = uL^d$. Close to the critical value $u = u_c$, many geometrical properties of the problem can be described as powers (critical exponents) of $u_c - u$, such as β , which controls the strength of the spanning cluster, and γ , which characterizes the behavior of the mean finite cluster size S . We show that at u_c the ratio between the mean mass of the largest cluster M_1 and the mass of the second largest cluster M_2 is independent of L and can be used to find u_c . We calculate β from the L dependence of M_1 and M_2 , and γ from the finite size scaling of S . The resulting exponent β remains close to 1 in all dimensions. The exponent γ decreases from ≈ 3.9 in $d = 3$ to ≈ 1.9 in $d = 4$ and ≈ 1.3 in $d = 5$ towards $\gamma = 1$ expected in $d = 6$, which is close to $\gamma = 4/(d - 2)$.

DOI: [10.1103/PhysRevE.110.024116](https://doi.org/10.1103/PhysRevE.110.024116)

I. INTRODUCTION

Percolation theory [1–3] provides a theoretical framework for several classes of theories describing generation of long-range connectivity from contacts between nearby objects. On regular lattices, these objects are sites or bonds. A group of connected neighboring sites or bonds forms a *cluster*. In this paper, we consider *site* percolation on hypercubic lattices. Such systems are characterized by a single parameter, such as the probability p of an occupied site. A cluster is *spanning* if it contains an uninterrupted path between opposing boundaries in a specific direction. In finite systems of linear size L , the probability $\Pi(p, L)$ of the existence of such a path gradually increases with increasing p . For an infinite system, $\Pi(p, \infty)$ becomes a step-function $\Theta(p - p_c)$ jumping from 0 to 1 at a particular *critical concentration* p_c . The mean spatial extent (linear size) of *finite* clusters is called the correlation length ξ . Close to p_c it diverges as

$$\xi \sim |p - p_c|^{-\nu}. \quad (1)$$

One of the simplest percolation models is Bernoulli site percolation on a d -dimensional lattice, where each lattice site is *independently* occupied with probability p . The exponent $\nu = \nu_B$ of this problem decreases with increasing d reaching $\nu_B = \frac{1}{2}$ for $d \geq d_c = 6$, i.e., at and above the *upper critical dimension* d_c [4]. Besides ν , the percolation problem is characterized by a large number of additional *critical exponents*, such as γ describing the divergence of the mean finite cluster size S (an accurate definition will be provided in the Sec. III) in the vicinity of p_c ,

$$S \sim |p - p_c|^{-\gamma}, \quad (2)$$

or the fraction of sites P belonging to the infinite cluster for $p > p_c$, also called the *strength* of the infinite cluster:

$$P \sim (p - p_c)^\beta. \quad (3)$$

For Bernoulli percolation, the values of these and other exponents are known exactly for $d = 2$ and $d \geq 6$, and have accurate numerical estimates for $d = 3, 4$, and 5 . There are numerous equalities relating various exponents describing the behavior close to the threshold, such as the hyperscaling relation

$$d\nu = 2\beta + \gamma \quad (4)$$

and others [1]. As a result, the values of many exponents can be deduced from only two exponents. Nevertheless, due to the limited accuracy of the numerical studies, additional exponents are measured and the values of the results are verified using the known relations.

In Sec. II, we define a correlated percolation model and briefly overview its properties as well as some known results. In Sec. III, we define the main quantities and briefly describe the numerical methods used in this paper. Section IV describes the properties of the largest clusters and their use to verify the position of the percolation threshold. Critical exponent β characterizing the strength of the infinite cluster is found from the L dependence of the first and the second largest clusters in Sec. V, while the exponent controlling the behavior of the mean cluster size γ is found in Sec. VI. Summary Sec. VII briefly discusses the results.

II. LONG-RANGE MODEL

Minor modifications of the Bernoulli percolation model, such as the introduction of short-range correlations between sites, consideration of bond percolation, or even power-law correlations $\sim 1/r^b$ between present sites at distance r with *large* power b do not change the critical behavior of the system

*Contact author: razhalifa@gmail.com

TABLE I. Some results of previous studies: First two columns show the space dimension d and the value of ν predicted by Weinrib [5], as applied to our problem [13] in Eq. (6), respectively. The 3rd and the 4th columns provide numerical estimates of ν and u_c from [13], while the last column gives the maximal linear size of a lattice used in that study.

d	ν_{th}	ν_{num}	u_c	L_{max}
3	2	2.04 ± 0.08	3.15 ± 0.01	512
4	1	1.0 ± 0.1	2.99 ± 0.01	64
5	$\frac{2}{3}$	0.65 ± 0.03	3.025 ± 0.008	32
6	$\frac{1}{2}$	~ 0.6	3.10 ± 0.05	16

[5]. However, if $b < 2/\nu_B$, then the correlations are relevant, and ν_B is replaced [5] by

$$\nu_{\text{long range}} = 2/b. \quad (5)$$

There is a variety of studies of correlated percolation models [6–12]. In this paper, we consider a problem where an initially full d -dimensional hypercubic lattice of linear size L (in lattice constants) and volume L^d has its sites removed by an \mathcal{N} -step random walk (RW) on the lattice. The *length* of the RW that starts at a random position is proportional to the *volume* of the lattice, namely, $\mathcal{N} = uL^d$. Periodic boundary conditions are imposed on the walk on a finite lattice, i.e., the walker exiting through one boundary of the lattice reemerges on the opposite boundary. The parameter u controls the length of the RW and the fraction p of unvisited sites. In repeated realizations of this process at fixed u , the average p is a monotonically decreasing function of u . For large L (and $d \geq 3$), there is a simple relation between these quantities: $p = \exp(-A_d u)$, where A_d are known constants (see Ref. [13] and references therein). An experimental realization of this model involves a gel of crosslinked polymers with the random walker represented by an enzyme that breaks the crosslinks between polymers that it encounters [14,15], eventually breaking the spanning cluster and turning the solid gel into a liquid. The object of our study is the sites *not visited* by the RW that represent the surviving crosslinks.

The variable u naturally replaces p in this problem, and p_c is replaced by the critical value u_c . (Keep in mind that the system percolates, i.e., has spanning clusters of unvisited sites *below* u_c .) In a previous study, it has been found that on hypercubic lattice for $3 \leq d \leq 6$ the threshold values $u_c \approx 3$ [13]. (See Table I.) This problem has been previously studied by Banavar *et al.* in $d = 2$ and 3 [16], while Abete *et al.* considered the critical behavior near the percolation threshold in $d = 3$ [17]. More recently, Kantor and Kardar studied the percolation properties of the problem for $2 \leq d \leq 6$ [13] and showed that the problem has no percolation threshold in $d = 2$ (for more details, see Ref. [18]). Recently, we received a work by Chalhoub *et al.* [19] with a detailed numerical study of the critical properties of this problem in large systems in $d = 3$ and analytical predictions regarding this problem and several similar problems in general d . We will compare their results with ours wherever it is appropriate.

Figure 1 depicts a typical configuration of the percolation of sites (blue cubes) not visited by a RW in $d = 3$. In this

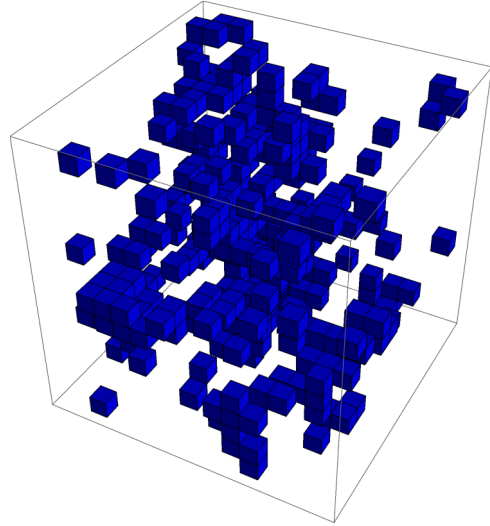


FIG. 1. Three-dimensional percolation in a small system of linear size $L = 16$. The sample was created by a random walk of $\mathcal{N} = uL^3$ steps, where $u = 4$. The blue cubes show the *unvisited* sites, which form several clusters. The visited sites form a single cluster.

realization, the number of steps of the RW exceeds four times the number of available lattice positions. Nevertheless, a significant fraction of the sites remains unvisited, since the RW frequently revisits previously visited sites. All *visited* sites form a *single cluster* since they have been created by a single RW. The unvisited sites form many clusters of various sizes. The picture is quite different from the usual geometries of Bernoulli percolation. The RW has a fractal dimension $\tilde{d}_f = 2$. On an *infinite* lattice, an \mathcal{N} -step walk explores distance $r \sim \mathcal{N}^{1/\tilde{d}_f} = \mathcal{N}^{1/2}$. Within that distance, the density of sites visited by the RW is $\mathcal{N}/r^d \sim 1/r^{d-2}$. On a *finite* lattice, a RW that exits through one boundary and re-enters through the opposite boundary creates almost uncorrelated strands, and the sites on different strands are no longer power-law correlated. A RW of length uL^d creates approximately uL^{d-2} such strands that contribute to an uncorrelated background density of sites. However, at distances r smaller than the lattice size, there remains a residual correlation of sites that happen to be on the *same* strand of the RW. Consequently, the *cumulant* of the correlation (from which the overall background density has been subtracted) still has $\sim 1/r^{d-2}$ correlation like a RW on an infinite lattice. Consider a random variable $v(\vec{x})$ which is 1 if the site at position \vec{x} is *unvisited* by the RW, and zero otherwise. It is complementary to the variable representing the *visited* site (their sum is 1) and therefore it has the same cumulant: $\langle v(\vec{x})v(\vec{y}) \rangle_c \sim 1/|\vec{x} - \vec{y}|^{d-2}$ [13]. Thus, the correlation power is $b = d - 2$, and the relation (5) becomes

$$\nu = 2/(d - 2), \quad \text{for } 3 \leq d \leq 6. \quad (6)$$

We note that, recently, Feshanjerdi *et al.* [20] studied a three-dimensional carbon copy version of our problem, where they considered percolation of sites *visited* by a (modified) RW. Their model is expected to have similar critical properties.

Kantor and Kardar's study of the problem in $3 \leq d \leq 6$ [13] focused on the behavior of the percolation probability $\Pi(u, L)$ as a function of RW parameter u and system size L . As L increases, $\Pi(u, L)$ approaches the step function $\Theta(u_c - u)$. Thus, by examining the u dependence of Π for a sequence of L values, it was possible to estimate the transition point u_c , while by studying L -dependence of the width of the transition between percolating ($\Pi \approx 1$) and nonpercolating ($\Pi \approx 0$) states it was possible to determine the exponent ν . Table I compares numerically calculated values of ν [13] with the predictions of Weinrib [5] in Eq. (6) and provides the calculated values of the thresholds. (In $d = 3$, an earlier estimate of ν on smaller systems ($L_{\max} = 60$) was 1.8 ± 0.1 [17], i.e., it slightly deviated from the predicted value of 2.) The conclusion of Ref. [13] was that the numerical results validated the theoretical prediction of Weinrib [5] in $d = 3, 4$, and 5, and we will use the theoretical values of ν in the current paper. (Dimension $d = 6$ is expected to be the upper critical dimension where $\nu = \frac{1}{2}$ coincides with ν_B of Bernoulli percolation. The system sizes in Ref. [13] were too small to reliably determine the value of the exponent.)

III. CLUSTERS AND FINITE-SIZE SCALING

In a system of N sites with N_s clusters containing s sites, we define *cluster density* $n_s \equiv N_s/N$. The total number of occupied sites on a lattice $M = \sum_s s N_s$, and therefore the fraction of occupied sites, is $p = M/N = \sum_s s n_s$. It is natural to define n_s and p as averages over an ensemble of systems, such as $n_s \equiv \langle N_s \rangle / N$, where $\langle \cdot \rangle$ defines ensemble average of "...". For simplicity of the notation, we will omit the $\langle \cdot \rangle$ signs where their presence is self-evident from the context. We also consider the thermodynamic limit of infinite lattices $N \rightarrow \infty$, where all n_s and p approach a finite limit. In an infinite lattice above the percolation threshold p_c , an infinite cluster is present and occupies some fraction $P > 0$ of the sites. Since summation over all integer numbers s does not include an infinite cluster, the $\sum_s s n_s = p - P$. (Below the threshold, $P = 0$ and the formula reduces to the expression that we had before.) In finite systems, the distinction between the would-be-infinite cluster and other clusters blurs and the transition itself is smeared. Therefore, it is customary [1] in numerical estimates of N_s on finite lattices to exclude the largest cluster of mass $s_{\max} \equiv M_1$ of any random realization of the system: For very large systems above p_c this is equivalent to the exclusion of the infinite cluster, while below p_c it slightly decreases the finite cluster size, but this effect decays with increasing L . Values of M_1 are used to estimate the fraction of the infinite cluster $P = M_1/N$. This procedure produces a nonvanishing effective P below the threshold, but its value decays to zero as the system size increases.

In infinite systems, the *second moment* $\chi \equiv \sum_s s^2 n_s$ characterizes the size (mass) of the *finite* cluster, since the sum excludes the infinite cluster, if such is present. In fact, the mean size S of a cluster to which a given occupied site belongs is given by $S = \chi / (p - P)$ [1]. [In an infinite system, both the mean cluster size S and the second moment χ diverge near p_c as shown in Eq. (2), and both can be used for numerical estimates of γ .] The expression for χ can be rewritten as $\chi = \sum_s s^2 N_s / N = \sum_\alpha s_\alpha^2 / N$, where the last sum simply rep-

resents a sum of squares of sizes of each distinct cluster α in the system. (In the finite systems in each configuration in our calculations, we exclude the largest cluster from that sum.)

For the problem of the sites unvisited by a RW, the system percolates *below* u_c and in all the expressions describing the behavior of S and P the arguments $p - p_c$ should be replaced by $u_c - u$, if the sign of the expression matters.

The second moment χ or the mean cluster size S are the geometrical analogs of the susceptibility in magnetic systems. In an infinite system near the threshold, Eq. (2) can be rewritten as $S \sim |u - u_c|^{-\gamma}$ and, similarly, Eq. (3) becomes $P \sim (u_c - u)^\beta$. The correlation length in Eq. (1) can be rewritten as $\xi \sim |u - u_c|^{-\nu}$. In a system of linear size L , the correlation length is naturally truncated by the system size and, consequently, S stops increasing when the expression for diverging ξ exceeds L . Similarly, P , which was supposed to vanish at u_c , abandons its power-law decay when $\xi \sim L$. In general, a critical quantity X that was supposed to be singular as $|u - u_c|^{-x}$, with either positive or negative exponent x becomes finite when $\xi > L$. It is also possible that the apparent position of the singularity (such as the position of the peak of S) may slightly differ from u_c and can be treated as an effective percolation threshold $u_c^*(L)$. (Its actual value may depend on the quantity which is being considered.) $u_c^*(L)$ keeps moving towards u_c with increasing L . It is expected that

$$|u_c - u_c^*(L)| \sim L^{-1/\nu}. \quad (7)$$

Finite-size scaling theory was originally developed for thermodynamic systems [21] and later adapted to percolation systems [1]. Since the behavior of the system is controlled by $\xi/L \sim |u - u_c|^{-\nu}/L$, it is convenient to describe the system by using parameter $v = (u - u_c)L^{1/\nu}$. In terms of v , the position of the peak of S becomes independent of L . When v is small, i.e., $|v| < V$, where V is some model-dependent number of order unity, the behavior of the system is controlled by the finite size L , while for $|v| \gg V$ we expect to recover infinite-system behavior. In general, the behavior of a critical quantity X can be described by

$$X = L^{x/v} g_X[L^{1/v}(u - u_c)] = L^{x/v} g_X(v), \quad (8)$$

where $g_X(v)$ is a scaling function. Thus, by drawing $XL^{-x/v}$ vs v with properly chosen parameters u_c , ν and x it should be possible to collapse all the results into a single curve, which is the function $g_X(v)$, as long as both L and ξ are significantly larger than the lattice constant. To recover the $L = \infty$ behavior $X \sim |u - u_c|^{-x}$, we must have $g_X(v) \sim |v|^{-x}$ for $|v| \gg V$. For small v the scaling function approaches some constant $g_X(0)$ leading to u -independent result $X \sim L^{x/v}$.

The numerical procedure used in this paper is rather straightforward: Initially, all sites on a hypercubic lattice L^d are present. The system sizes in $d = 3$ are $L = 16, 32, 64, \dots, 512$. For $d = 4$, they are 16, 32, 64, and 128, while in $d = 5$ the L s are increased by approximately factor $\sqrt{2}$: 16, 23, 32, 45. These L s are slightly larger than in the previous study (see Table I). A RW starts at a randomly selected site and for a given u performs uL^d steps removing the sites that have been visited. At each realization, the Hoshen-Kopelman algorithm [22] is used to identify *all* clusters, and from the complete list of clusters all necessary quantities characterizing that configuration can be calculated. For a fixed u and L , this

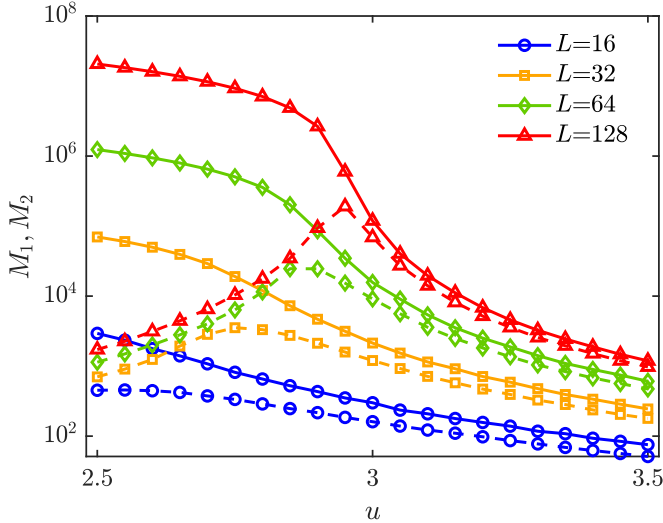


FIG. 2. Semilogarithmic plot of the mean mass M_1 of the largest cluster (solid lines) and the mean mass M_2 of the second largest cluster (dashed lines) as a function of RW parameter u , in $d = 4$ for (bottom to top) $L = 16$ (blue circles), 32 (yellow squares), 64 (green diamonds), and 128 (red triangles). Here, as in other graphs, each point represents an average over 1000 configurations. Relative statistical errors in M_1 and M_2 are $\lesssim 4\%$, which on logarithmic scale results in error bars $\Delta \log_{10} M_2 \lesssim 0.02$ which are smaller than the symbol sizes. Horizontal separation between data points $\Delta u = 0.05$. Qualitatively similar behavior was observed in $d = 3$ and $d = 5$.

RW procedure is repeated 1000 times and various quantities are averaged over the realizations. For each L , a sequence of us is studied to obtain u dependence of such averages at typical steps $\Delta u = 0.05$, except for specific situations mentioned in the text.

IV. TWO LARGEST CLUSTERS

At any d , on a finite lattice of linear size L the typical mass (number of sites) M_1 of the *largest* cluster has a very different u dependence than the mass M_2 of the *second largest* cluster: In the percolating region ($u < u_c$), M_1 is essentially the mass of the would-be-infinite cluster PL^d . For a very small u , we have $M_1 \approx L^d$ and it decreases with increasing u . For $u > u_c$ in the nonpercolating region, M_1 is just the largest of the finite clusters that are present and it keeps decreasing with increasing u . So, overall, M_1 is a monotonically decreasing function of u . For a very small u , almost all space is occupied by the massive spanning cluster, and $M_2 \approx 1$. As u increases (still in the percolating region), so do the sizes of finite clusters and M_2 increases. Above u_c , the typical cluster sizes decrease with increasing u and so does the mass M_2 . In that region, it has a similar behavior to M_1 but, obviously, is smaller than M_1 . We expect M_2 to have a maximum somewhere around u_c . Figure 2 shows M_1 and M_2 for several system sizes L in $d = 4$. (Similar behavior is found at other ds .) Indeed, M_1 is a monotonically decreasing function, while M_2 has a maximum at some $u_c^*(L)$, which approaches u_c with increasing L as in Eq. (7).

At the percolation threshold, the largest cluster has fractal structure, and its mass increases with the system size

as $M_1 \sim L^{d_f}$ [1], where d_f is the fractal dimension of the infinite cluster. However, it has been known for quite some time [23–25] that for Bernoulli percolation at the threshold, the mass of the *second* largest cluster M_2 (as well as third and higher rank clusters) also scales with the same power, although it has a smaller prefactor. Therefore, one can expect that the *ratios* of two such cluster masses, represented either by the ensemble average $\langle M_1/M_2 \rangle$ or by $\langle M_1 \rangle / \langle M_2 \rangle$ will scale with the zeroth power of L . So, this ratio can be treated using the same finite-size arguments that were used for X and lead to scaling form (8), with $x = 0$ and a different scaling function [26] g_0 . While this reasoning originally applied to Bernoulli percolation, it originates from the argument that at a critical point in the absence of length scale, both the largest and the second largest clusters share the same behavior. Therefore, this property can be expected (subject to verification) in our correlated percolation problem. In such a case, we expect

$$\langle M_1/M_2 \rangle \text{ or } \langle M_1 \rangle / \langle M_2 \rangle = g_0[L^{1/\nu}(u - u_c)] = g_0(v). \quad (9)$$

At $u = u_c$ this equation means that the ratio of masses of the first and the second largest clusters at the critical point should be $g_0(0)$, i.e., independent of L . The presence of such an intersection at u_c both confirms that the first and the second largest clusters have the same fractal dimension, and enables an alternative approach for an accurate determination of the percolation threshold. This method has been successfully used by da Silva *et al.* [27] to locate p_c in Bernoulli percolation problem.

The study in Ref. [13] of correlated percolation extracted the value of u_c by examining the percolation probability $\Pi(u, L)$ as a function of u for several values of L , and observing the approach of that function to the infinite- L limit of step function $\Theta(u_c - u)$. With increasing u , the function $\Pi(u, L)$ monotonically decreases from a percolating small- u regime to a nonpercolating large- u region. The effective transition point \tilde{u} was defined as a point where $\Pi(\tilde{u}, L) = c$, with an arbitrary constant $0 < c < 1$. Clearly, the value of \tilde{u} depends both on L and c . Since in the $L \rightarrow \infty$ limit the Π becomes a step function, in that limit $\tilde{u} \rightarrow u_c$ independently of the choice of c . Indeed, in Ref. [13] it was shown that various choices of c lead to similar $L \rightarrow \infty$ extrapolations. However, all \tilde{u} values exhibited significant L dependence, and therefore it is beneficial to use an alternative method to confirm that threshold values appearing in Table I. We apply the method of da Silva *et al.* [27] to our problem. Figure 3 depicts the u dependence of M_1/M_2 for various values of L in $d = 4$. We note that the intersection points between various lines are concentrated between 2.99 and 3.00, even for moderate Ls , similar to $u_c = 2.99 \pm 0.01$ that has been obtained by strong extrapolations in Ref. [13]. (We will use value of $u_c = 2.995$ for the fits in $d = 4$ in the remainder of the paper.)

We performed similar studies of M_1/M_2 in $d = 3$ and $d = 5$ and confirmed the known values of u_c listed in Table I. (Fig. 1 in Ref. [19] uses an analogous method of line-intersection for different types of quantities to determine u_c in $d = 3$ and concludes that our original value $u_c = 3.15$ was correct.) We will use the u_c values from Table I (for $d = 3$ and 5) in the remainder of this paper. While the results obtained in the following sections require the knowledge of u_c , they

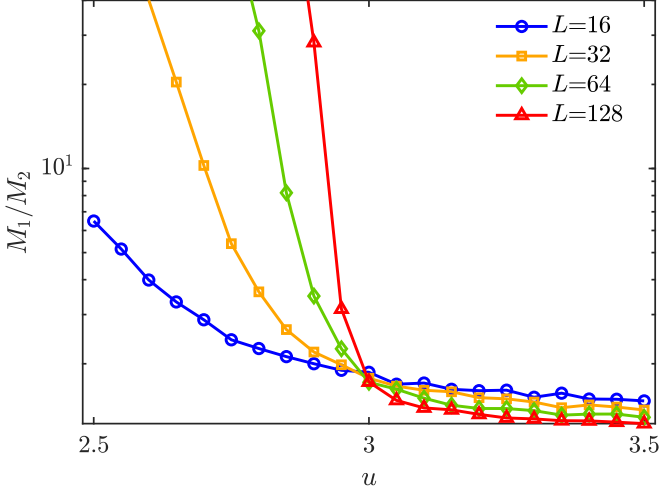


FIG. 3. Semilogarithmic plot of the ratios of mean mass M_1 of the largest cluster and the mean mass M_2 of the second largest cluster as a function of RW length parameter u in $d = 4$ for system sizes (left to right on the top parts of the graphs) $L = 16$ (blue circles), 32 (yellow squares), 64 (green diamonds), and 128 (red triangles). This figure uses the same data as Fig. 2 and shares the same technical details. The intersection points of subsequent- L lines are between 2.99 and 3.00 and provide an estimate for u_c (Smaller Δu s were used close to u_c but the extra data points are not shown here.) Qualitatively similar behavior was observed in $d = 3$ and $d = 5$.

are rather insensitive to its exact value and even changes in the values of u_c as large as 0.01 or 0.02 do not modify the estimates of the critical exponents.

V. EXPONENT β

Critical exponent β is defined by the behavior of the infinite cluster P near the percolation threshold, i.e., in an infinite system $P \sim (u_c - u)^\beta$ for $u < u_c$. One can directly plot measured P vs $u_c - u$ on a logarithmic plot for a sequence of increasing L s, and determine the exponent β . For a finite L , the power law is truncated when ξ reaches L , and it is possible to treat that truncation more systematically by considering a finite-size scaling form for P which is analogous to Eq. (8),

$$P = L^{-\beta/v} g_P[L^{1/v}(u - u_c)] = L^{-\beta/v} g_P(v), \quad (10)$$

where $g_P(v)$ is a scaling function, which for large *negative* v should have the behavior $g_P(v) \sim (-v)^\beta$ to recover the desired L -independent behavior of P , while for small v we obtain u -independent result $P \sim L^{-\beta/v}$. Since P is small close to u_c , it increases the relative statistical errors and reduces the accuracy of the numerical calculations near that point. On the other hand, one can concentrate on a fixed v , such as $v = 0$, and explore the relation $P = L^{-\beta/v} g_P(0)$. Since $P = M_1/L^d$, we may use the relation $M_1 \sim L^{d_f}$, with the fractal dimension

$$d_f = d - \beta/v. \quad (11)$$

Since both M_1 and M_2 have the same fractal dimension at u_c , by plotting both $M_1(v = 0)$ and $M_2(v = 0)$ as a functions of L on a logarithmic scale, one can determine d_f and, consequently, the exponent β . The solid lines in Fig. 4 depict on a logarithmic scale the dependence of M_2 at u_c on system size

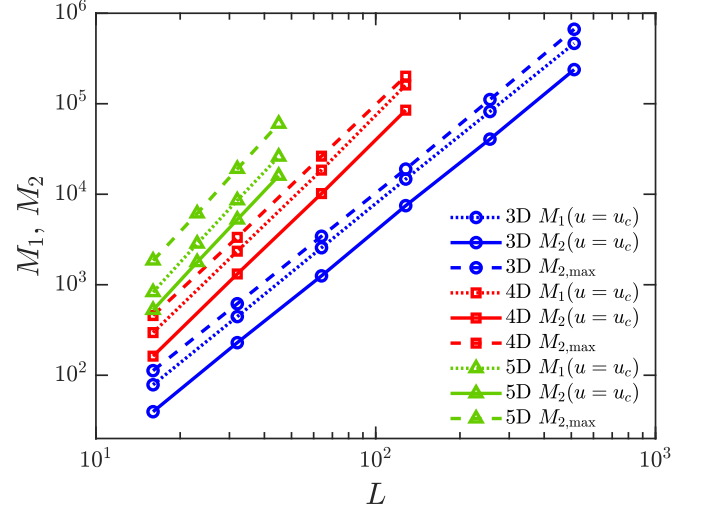


FIG. 4. Logarithmic plots of the mean mass M_1 of the largest cluster measured at u_c ($v = 0$) (dotted lines) and of the mean mass M_2 of the *second* largest cluster measured at u_c ($v = 0$) (solid lines) or at the maximum of the curve ($v = v_{\max}$) (dashed lines) as a function of L for (bottom to top triplets of lines) $d = 3$ (blue circles), $d = 4$ (red squares), and $d = 5$ (green triangles). Each data point depicts an ensemble average and the error bars, as explained in Fig. 2, are smaller than the symbol sizes. Slopes of the curves are the fractal dimensions d_f of the clusters.

L in the complete range of L s used for each $d = 3, 4$, and 5 . From the slopes of the lines (d_f) and from Eq. (11), we deduce $\beta = 0.98 \pm 0.04$ in $d = 3$, $\beta = 1.00 \pm 0.06$ in $d = 4$, and $\beta = 1.09 \pm 0.05$ in $d = 5$. Similarly, the dotted lines depict the values of M_1 from which we deduce $\beta = 0.99 \pm 0.02$ in $d = 3$, $\beta = 0.98 \pm 0.10$ in $d = 4$, and $\beta = 1.11 \pm 0.07$ in $d = 5$. The stated errors combine small statistical errors of individual M_1 or M_2 data points (relative errors smaller than 4%) with the scatter of the points around the straight line. We could not determine a systematic L dependence of the slope, which might indicate that we are measuring an effective exponent which changes with increasing L . If such a change was present, it was masked by the statistical fluctuations of the slope.

The result for $d = 3$ should be compared with the result $\beta = 1.0 \pm 0.1$ of Abete *et al.* [17] obtained on smaller systems ($L_{\max} = 60$). (In that calculation, a slightly smaller value of v was used.) Our result in $d = 3$ is also consistent (within quoted errors) with the result obtained in Ref. [19] for larger systems ($L_{\max} = 600$). A similar result was also obtained by Feshanjerdi *et al.* [20] for a problem of *visited* sites; they conjectured that the exact value of β in $d = 3$ should be the integer value 1. Table II displays previously calculated values of β and other exponents in $d = 3$ by several authors. Note that our β values in $d = 3$ are consistent with the previously known values.

As an additional check of the presence or absence of systematic errors, we measured M_2 at its maximal value. We verified that, within statistical uncertainty, the maximal values of M_2 for all L appear at the same value of v_{\max} . This is correct for each d , although the actual definition of v depends on d since it involves specific u_c and v . Thus, the measurement

TABLE II. Numerical values of exponents from previous studies of percolation of sites or bonds *not visited* by a RW in $d = 3$. The fifth column provides the source reference, while the fourth column gives the maximal linear size of a lattice used in that study. (This table excludes the results appearing on the first line of Table I.) Asterisks indicate results for a (presumably equivalent) model of sites *visited* by a modified RW. The values of β or γ are frequently calculated as the ratios β/v_{num} or γ/v_{num} , respectively, and have been calculated from the results appearing in the references. Some authors used several methods to calculate the same exponents, and the reader should consult the original references.

v_{num}	β	γ	L_{max}	Ref
1.8 ± 0.1	1.0 ± 0.1	3.5 ± 0.2	60	[17]
$1.99 \pm 0.01^*$	$0.99 \pm 0.01^*$		1024	[20]
1.95 ± 0.11		4.00 ± 0.36	600	[19]
2.02 ± 0.08	0.98 ± 0.08			

of $M_2(v = v_{\text{max}})$ for various L s should produce the same L -dependence $M_2 \sim L^{d_f}$, although with a larger prefactor, as we got for $v = 0$ (or $u = u_c$). This method of measurement introduces an additional source of errors, since finding maximal M_2 requires interpolation between data points close to that maximum. The presence of this additional error increases in the estimated statistical errors. Dashed lines in Fig. 4 depict M_2 as a function of L measured at the points of maxima. The measured slopes (d_f) produce slightly different values: $\beta = 0.99 \pm 0.07$ in $d = 3$, $\beta = 1.07 \pm 0.06$ in $d = 4$, and $\beta = 1.13 \pm 0.05$ in $d = 5$. While the results at $v = v_{\text{max}}$ are less reliable, they are similar to the previous sets of β s.

The study of the behavior of M_1 and M_2 , demonstrated in this section supports the extension of the scaling form in Eq. (10) to M_i ($i = 1, 2$), namely,

$$M_i = L^{d_f} g_{M_i}[L^{1/\nu}(u - u_c)] = L^{d_f} g_{M_i}(v), \quad (12)$$

where $g_{M_i}(v) \equiv g_P(v)$. Figure 5 demonstrates such scaling via data collapse of scaled M_1 and M_2 for various L s for $d = 4$. [In this graph, as well as in other scaled plots (the last two figures of the paper) instead of sampling the functions at fixed intervals Δu , we use (almost) fixed intervals Δv of the scaled variable.] We note that the value of β used in this fit is in the middle of β values obtained from Fig. 4 for the same d . Analogous behavior is observed in other dimensions.

As mentioned at the beginning of this section, the behavior of $g_P(v)$ for *large* negative v is consistent with the expected power law but is not accurate enough to determine the value of β .

We note that in $d = 6$, the exponent of our problem should coincide with the exponent of Bernoulli percolation and have mean field value $\beta = 1$. The fact that β maintains the value so close to 1 in all dimensions makes one wonder if $\beta = 1$ is the exact dimension-independent value of β . Such conjecture has been made by Feshanjerdi *et al.* [20] in $d = 3$ (for a system of visited sites) and theoretically suggested to be valid in other dimensions by Chalhoub *et al.* [19] (see Table I in their work).

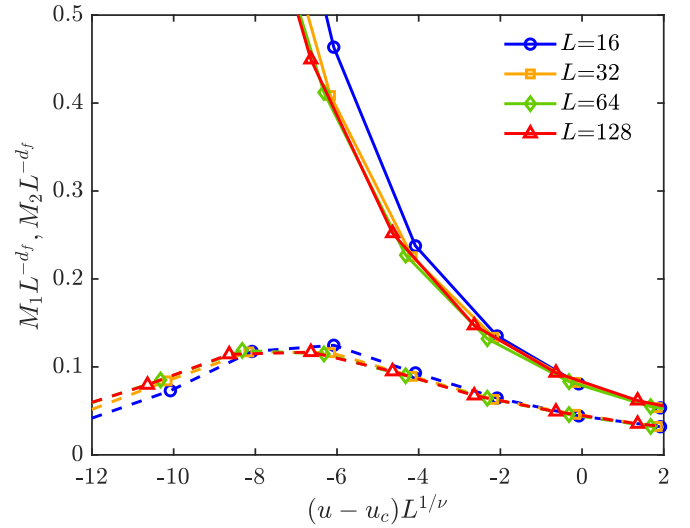


FIG. 5. Data-collapse plot of the scaled cluster sizes $M_1 L^{-d_f}$ (top solid lines) and $M_2 L^{-d_f}$ (bottom dashed lines) in $d = 4$ vs scaled parameter $v = (u - u_c)L^{1/\nu}$. This graph was obtained for d_f with $\beta = 1.04$ [see Eq. (11)] and it remains a good fit when β is changed by ± 0.04 . This graph is a scaled form of Fig. 2. The error bars are smaller than the sizes of the symbols.

VI. EXPONENT γ

Mean cluster size S is one of the most important characteristics of percolation. In infinite systems, similarly to the susceptibility in magnetic systems, it diverges at the critical point as in Eq. (2), and it would be possible to measure the exponent γ by directly plotting S as a function of the distance from the critical point on a logarithmic scale. (Exponent γ is expected to be the same both above and below that point.) However, in a finite system, the divergence is truncated when ξ exceeds L . Figure 6 depicts S measured in $d = 3$ as a function of u for system sizes L ranging from 16 to 512. As L increases, the height of the peak in S increases approximately as L^2 . The position of the peak appears at some $u_c^*(L)$, which is smaller than u_c and this effective critical point shifts towards u_c with increasing L as indicated by Eq. (7), while the height of the peak increases almost as L^2 . As with other critical quantities, we will use scaled variable $v = (u - u_c)L^{1/\nu}$ and describe the behavior of S using scaling form analogous to Eq. (8), namely,

$$S = L^{\gamma/\nu} g_S[L^{1/\nu}(u - u_c)] = L^{\gamma/\nu} g_S(v), \quad (13)$$

where $g_S(v)$ is a scaling function. To recover the $L = \infty$ behavior $S \sim |u - u_c|^{-\gamma}$, we must have $g_S(v) \sim |v|^{-\gamma}$ for $|v| \gg V$. For small v , the scaling function approaches some constant $g_S(0)$, leading to u -independent result $S \sim L^{\gamma/\nu}$. Instead of focusing on $v = 0$, we can look at a point $v = v_{\text{max}}$, where all S reach their maxima independently of L . At this point, we also expect $S \sim L^{\gamma/\nu}$ but with a larger prefactor. In fact, the exponent γ can be determined from the entire function $g_S(v)$: We need to plot $SL^{-\gamma/\nu}$ vs v . Such a plot should produce the function $g_S(v)$. The graphs for several L s should collapse into a single plot, provided the fitting parameter $\gamma \equiv \gamma/\nu$ has been properly selected. In general, we should use three fit parameters γ , ν and u_c . However, the latter two

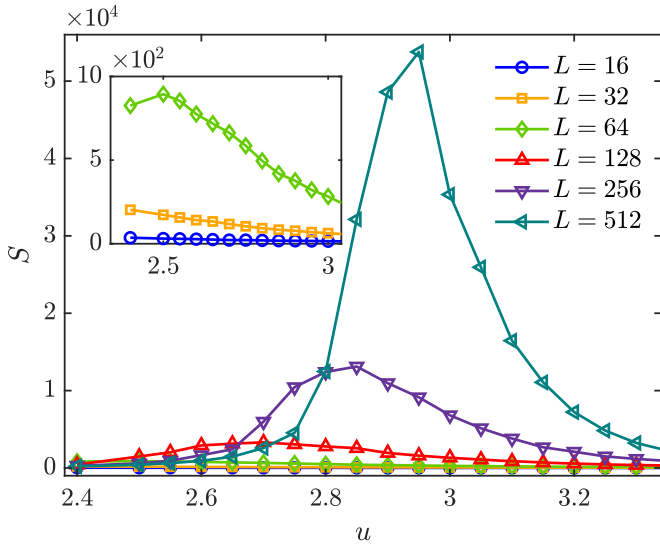


FIG. 6. Mean cluster size S vs u in $d = 3$ for $L = 16, 32, \dots, 512$. Error bars are smaller than the symbols. The inset shows the graphs for the three smallest L s with an expanded vertical scale. The expected critical point is $u_c = 3.15$, while the maxima of the curves appear at slightly lower values $u_c^*(L)$ that drift towards u_c with increasing L .

are well-known to us—see Table I. (The fitting is insensitive to small changes in u_c .) We therefore use the known values of $\nu = \nu_{th} = 2$ and $u_c = 3.15$ from Table I and adjust only the parameter γ that depends on γ . Using the above values, Fig. 7 presents the same results as Fig. 6 in a scaled form where the horizontal axis uses variable $v = (u - u_c)L^{1/\nu}$. The vertical axis represents the scaled cluster size $SL^{-\gamma}$, with the fit parameter γ corresponding to $\gamma = 3.90$. The fit remains good up to a shift of ± 0.05 in γ . Note that the best-fit value of γ is very close to 2. The obtained value of γ should be compared

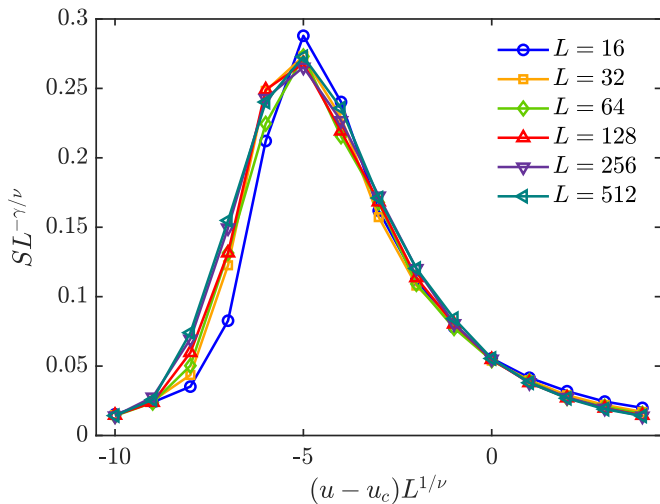


FIG. 7. Data-collapse plot of the scaled mean cluster size $SL^{-\gamma}$ in $d = 3$ vs scaled parameter $v = (u - u_c)L^{1/\nu}$. This graph was obtained for $\gamma = \gamma\nu = 3.90$ and it remains a good fit when γ is changed by ± 0.05 . This graph is a scaled form of Fig. 6. The error bars are smaller than the sizes of the symbols.

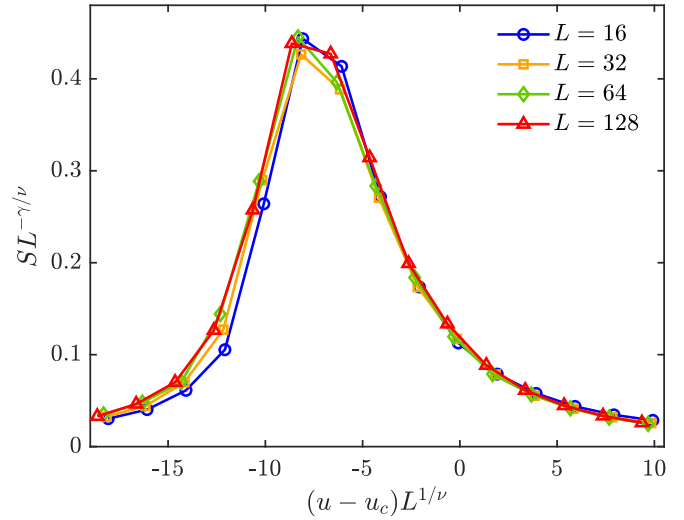


FIG. 8. Data-collapse plot of the scaled mean cluster size $SL^{-\gamma}$ in $d = 4$ vs scaled parameter $v = (u - u_c)L^{1/\nu}$. It is analogous to $d = 3$ graph in Fig. 7. The exponent γ was adjusted to get the best data collapse. This graph was obtained for $\gamma = \gamma\nu = 1.90$ and it remains a good fit when γ is changed by ± 0.05 . The error bars are smaller than the symbol sizes.

with $\gamma \approx 3.5$ by Abete *et al.* [17] obtained on smaller systems ($L_{max} = 60$) and with a slightly smaller numerical value of ν , and $\gamma \approx 4.0$ obtained by Chalhoub *et al.* [19] on a slightly larger system. (See previous results in Table II.)

Our result was extracted from the behavior for small v behavior of $g_S(v)$. As expected, for large $|v|$ we observe a power law which is consistent with $|v|^{-\gamma}$, but the quality and the range of the data is too small for an accurate determination of the power.

We repeated the above calculations in $d = 4$ and $d = 5$. The decreasing range of L leads to decreasing reliability of the fit. As an example, we present Fig. 8 that shows the scaled results in $d = 4$, for L ranging from 16 to 128. By fitting γ , we find $\gamma = 1.90 \pm 0.05$, and again parameter γ is very close to 2. Similar analysis was performed in $d = 5$ on systems of even smaller linear size L ranging from 16 to 45. The collapse plot (not shown) has slightly lower quality and the best fit leads to the estimate $\gamma = 1.30 \pm 0.05$.

As in the three-dimensional case we compared the values of γ obtained for small values of v with possible power-law behavior $|v|^{-\gamma}$. Again, we obtained a reasonable correspondence for large negative values of v , although the accuracy of those results was much lower. (We did not see a clear power law for large positive v .)

We expect the exponents β obtained in the previous section and the exponents γ obtained in this section to satisfy the hyperscaling relation (4). Indeed, by inserting the calculated values the relation is approximately satisfied if we allow for errors in the exponents. In fact, we can use (4) in an opposite way: if we substitute $\beta = 1$ into the equation and use ν from (6) we find that in our problem

$$\gamma = 4/(d - 2). \tag{14}$$

We can see that this expression is very close to the values of γ obtained in all dimensions. [We also note that (14) leads for all $3 \leq d \leq 6$ to the exponent $y = \gamma/\nu = 2$.]

VII. DISCUSSION

The problem of sites not visited by a RW presents a relatively simple case of correlated percolation. In this paper,

we calculated exponents β and γ in $d = 3, 4$, and 5 , with reasonable accuracy, using system sizes comparable with the previous works. (There were no previous results in $d = 4$ and 5 .) We used different methods to measure the exponents: measurement of the fractal dimension of the first and the second largest clusters for calculation of β and finite size scaling for γ . Our results hint at simple numerical values for the critical exponents, and one may hope to derive these values from simple geometrical considerations.

-
- [1] D. Stauffer and A. Aharony, *Introduction to Percolation Theory*, 2nd ed. (Taylor and Francis, London, 1991).
- [2] G. Gremmett, *Percolation*, 2nd ed. (Springer, Berlin, 1999).
- [3] A. A. Saberi, Recent advances in percolation theory and its applications, *Phys. Rep.* **578**, 1 (2015).
- [4] G. Toulouse, Perspectives from the theory of phase transitions, *Nuov. Cim. B* **23**, 234 (1974).
- [5] A. Weinrib, Long-range correlated percolation, *Phys. Rev. B* **29**, 387 (1984).
- [6] A. Coniglio and A. Fierro, Correlated percolation, in *Encyclopedia of Complexity and Systems Science* (Springer, New York, 2009), Part 3, pp. 1596–1615.
- [7] G. Gori, M. Michelangeli, N. Defenu, and A. Trombettoni, One-dimensional long-range percolation: A numerical study, *Phys. Rev. E* **96**, 012108 (2017).
- [8] O. Riordan and L. Warnke, Explosive percolation is continuous, *Science* **333**, 322 (2011).
- [9] R. M. D’Souza and J. Nagler, Anomalous critical and supercritical phenomena in explosive percolation, *Nat. Phys.* **11**, 531 (2015).
- [10] Y. Kantor, Three-dimensional percolation with removed lines of sites, *Phys. Rev. B* **33**, 3522 (1986).
- [11] K. J. Schrenk, N. Posé, J. J. Kranz, L. V. M. van Kessenich, N. A. M. Araujo, and H. J. Herrmann, Percolation with long-range correlated disorder, *Phys. Rev. E* **88**, 052102 (2013).
- [12] K. J. Schrenk, M. R. Hilário, V. Sidoravicius, N. A. M. Araújo, H. J. Herrmann, M. Thielmann, and A. Teixeira, Critical fragmentation properties of random drilling: How many holes need to be drilled to collapse a wooden cube? *Phys. Rev. Lett.* **116**, 055701 (2016).
- [13] Y. Kantor and M. Kardar, Percolation of sites not removed by a random walker in d dimensions, *Phys. Rev. E* **100**, 022125 (2019).
- [14] H. Berry, J. Pelta, D. Lairez, and V. Larreta-Garde, Gel-sol transition can describe the proteolysis of extracellular matrix gels, *Biochim. Biophys. Acta* **1524**, 110 (2000).
- [15] G. C. Fadda, D. Lairez, B. Arrio, J.-P. Carton, and V. Larreta-Garde, Enzyme-catalyzed gel proteolysis: an anomalous diffusion-controlled mechanism, *Biophys. J.* **85**, 2808 (2003).
- [16] J. R. Banavar, M. Muthukumar, and J. F. Willemsen, Fractal geometries in decay models, *J. Phys. A: Math. Gen.* **18**, 61 (1985).
- [17] T. Abete, A. de Candia, D. Lairez, and A. Coniglio, Percolation model for enzyme gel degradation, *Phys. Rev. Lett.* **93**, 228301 (2004).
- [18] A. Federbush and Y. Kantor, Percolation perspective on sites not visited by a random walk in two dimensions, *Phys. Rev. E* **103**, 032137 (2021).
- [19] C. Chalhoub, A. Drewitz, A. Prévost, and P.-F. Rodriguez, Universality classes for percolation models with long-range correlations, [arXiv:2403.18787](https://arxiv.org/abs/2403.18787).
- [20] M. Feshanjerdi, A. A. Masoudi, P. Grassberger, and M. Ebrahimi, Aftermath epidemics: Percolation on the sites visited by generalized random walk, *Phys. Rev. E* **108**, 024312 (2023).
- [21] V. Privman and M. E. Fisher, Universal critical amplitudes in finite-size scaling, *Phys. Rev. B* **30**, 322 (1984).
- [22] J. Hoshen and R. Kopelman, Percolation and cluster distribution. I. Cluster multiple labeling technique and critical concentration algorithm, *Phys. Rev. B* **14**, 3438 (1976).
- [23] A. Margolina, H. J. Herrmann, and D. Stauffer, Size of largest and second largest cluster in random percolation, *Phys. Lett. A* **93**, 73 (1982).
- [24] N. Jan, D. Stauffer, and A. Aharony, An infinite number of effectively infinite clusters in critical percolation, *J. Stat. Phys.* **92**, 325 (1998).
- [25] N. Jan, Large lattice random site percolation, *Physica A* **266**, 72 (1999).
- [26] C. R. da Silva, M. L. Lyra, and G. M. Viswanathan, Boundary condition dependence of cluster size ratios in random percolation, *Int. J. Mod. Phys. C* **11**, 1411 (2000).
- [27] C. R. da Silva, M. L. Lyra, and G. M. Viswanathan, Largest and second largest cluster statistics at the percolation threshold of hypercubic lattices, *Phys. Rev. E* **66**, 056107 (2002).